

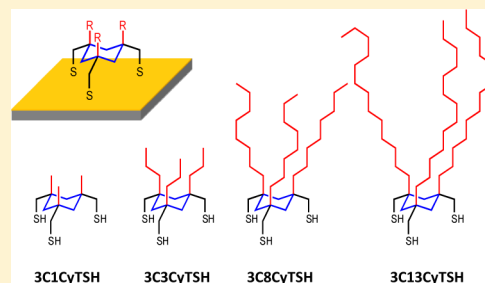
# Self-Assembled Monolayer Films Derived from Tridentate Cyclohexyl Adsorbates with Alkyl Tailgroups of Increasing Chain Length

Burapol Singhana, Andrew C. Jamison, Johnson Hoang, and T. Randall Lee\*

Department of Chemistry and the Texas Center for Superconductivity, University of Houston, Houston, Texas 77204-5003

## Supporting Information

**ABSTRACT:** Tridentate cyclohexyl-based alkanethiolate SAMs generated from a series of adsorbates of the form  $R_3C_6H_6(CH_2SH)_3$ , where  $R = -(CH_2)_nH$  and  $n = 3, 8,$  and  $13$  (**3CnCyTSH**), were examined. Characterization of the SAMs by X-ray photoelectron spectroscopy (XPS) revealed that all sulfur atoms of the tridentate adsorbates were bound to the surface of gold, and that the tailgroups were in general less densely packed than the SAM derived from octadecanethiol (**C18SH**). For each of the SAMs, the relative molecular coverage on the surface was estimated from the XPS-derived  $C_{1s}/Au_{4f}$  ratios. The trend in conformational order for these SAMs as determined by the surface interactions with contacting liquids and the relative crystallinity of the alkyl chains as revealed by the PM-IRRAS spectra were found to decrease as follows: **C18SH**  $\gg$  **3C13CyTSH**  $>$  **3C8CyTSH**  $>$  **3C3CyTSH**. A preliminary study of the thermal stability of the SAMs as evaluated by XPS indicates that the SAM generated from the cyclohexyl-based adsorbate with the longest alkyl chain, **3C13CyTSH**, is markedly more stable than the SAM generated from **C18SH**. Overall, the results suggest that the stability of the SAMs are influenced by both the length of the alkyl chains and the chelate effect associated with the tridentate adsorbates.



## INTRODUCTION

Self-assembled monolayers (SAMs) of organic alkanethiols on gold have been used in the design and controlled fabrication of nanostructured materials such as soft lithography resists,<sup>1</sup> biosensors,<sup>2</sup> nanoparticles for drug delivery,<sup>3</sup> thin-film organic electronic devices,<sup>4</sup> nanoscale coatings,<sup>5</sup> and a variety of other purposes.<sup>6,7</sup> Although alkanethiolate monolayers have received considerable interest in the scientific community, the stability of these thin films is still a significant obstacle for their use in real-world applications.<sup>8–14</sup> In particular, these organic thin films exhibit only moderate stability under ambient conditions<sup>10,14</sup> and decompose rapidly at elevated temperatures (e.g.,  $\sim 80$  °C in hexadecane).<sup>8,11–13</sup> Previous studies have also found that certain thiol adsorbates partially desorb upon exposure to air overnight<sup>14</sup> and most readily undergo displacement when exposed to a second organosulfur adsorbate in solution.<sup>10,11</sup>

A variety of strategies have been devised by a number of surface scientists to enhance the stability of these organic thin films; these include interchain cross-linking and adsorbate polymerization,<sup>15–18</sup> multiple sulfur–gold interactions (chelation by multidentate adsorbates),<sup>13,19–28</sup> and intermolecular hydrogen bonding.<sup>29–31</sup> Of particular interest are the multidentate adsorbates with three surface bonds that enable the production of stable SAMs utilizing the “chelate effect”.<sup>13</sup> Such tridentate architecture was initially reported by Whitesell et al. in 1993 for research involving the growth of helical peptides from gold surfaces.<sup>27</sup> But the number of applications has broadened for these unique surfactants, as detailed in recent reviews.<sup>11,12</sup>

Our research group has been exploring the formation and characterization of SAMs on polycrystalline “flat” gold and on gold nanoparticles derived from the adsorption of various multidentate alkanethiols.<sup>11–13,19–24,32,33</sup> As a whole, we found that SAMs generated from tridentate adsorbates are more thermally stable than those generated from bidentate adsorbates, which in turn are more stable than those generated from monodentate adsorbates.<sup>33</sup> Furthermore, independent studies have found that long-chain alkanethiols fail to displace tridentate adsorbates under conditions where monodentate adsorbates were readily displaced.<sup>28</sup> Of particular relevance to this report, adamantane-based tridentate adsorbates have been previously developed and used to generate SAMs on gold.<sup>27,34–37</sup> For these adsorbates, all three thiomethyl legs extend from a single cyclohexane ring of the framework of these rigid cage-like structures and bind to gold in a fashion similar to normal alkanethiols.<sup>36–38</sup> However, there have been no reports of more extensive studies of the stability of the films generated from these trithiol adsorbates.

In a recent publication,<sup>39</sup> we provided our initial assessment of SAMs formed from simple cyclohexyl-based tridentate adsorbates. In this initial investigation, two trithiols built with this architecture were synthesized and used to prepare thin films on gold (see Figure 1), **CyTSH** and **3C1CyTSH**, where  $R = -CH_3$  in the illustration. Our studies revealed that while the adsorption of **CyTSH** led to multilayer films containing

Received: May 19, 2013

Revised: October 2, 2013

Published: October 7, 2013

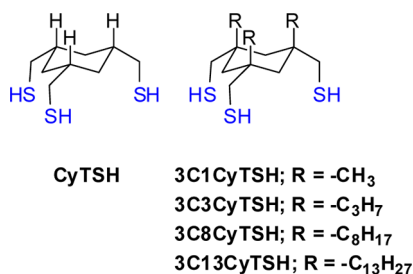


**Figure 1.** Illustration of the structure of the cyclohexyl-based trithiol adsorbates.

oxidized sulfur species, the adsorption of **3C1CyTSH** led to monolayer films with  $\sim 90\%$  of the sulfur atoms bound to gold. The striking difference between these two adsorbates can be attributed to the presence of the methyl groups in **3C1CyTSH**, which restrict the conformational flexibility of the cyclohexane ring and thereby significantly enhance its chemisorption to gold. The results suggest that derivatives of the **3C1CyTSH** architecture might be used to generate strongly bound SAMs on gold.

On the basis of these earlier results, we chose to further explore this new chemical architecture with the goal of developing a more versatile class of multidentate adsorbate that would produce stable, well-defined SAMs on gold. To this end, we synthesized three new analogs of **3C1CyTSH** having the general formula  $R_3C_6H_6(CH_2SH)_3$ , where  $R = -(CH_2)_nH$  and  $n = 3, 8,$  and  $13$  (**3CnCyTSH**; see Figure 1). With the **3CnCyTSH** adsorbates, the cyclohexane ring serves as the platform between the three alkyl tailgroups and the three thiol-containing headgroups. By varying the length of the pendant alkyl chains, we wished to determine the degree to which this parameter influences the formation, structure, and stability of SAMs derived from these unique adsorbates. Specifically, we anticipated that the chain length would influence the efficiency of the bonding to the surface, the packing density of the tailgroups, and the stability of the films. Even though **3C1CyTSH** forms SAMs with  $\sim 90\%$  of the thiols bound to gold, the alkyl chain is too short to affect the packing characteristics of these SAMs due to small interchain van der Waals interactions. Therefore, we anticipated that analogs of **3C1CyTSH** having longer chain lengths would yield an increased surface packing density for the adsorbates and, consequently, an enhanced stability for the SAMs. Studies of SAMs created from this new class of adsorbate should further advance our understanding of the structural factors that lead to stable SAMs on gold. Moreover, this new tridentate architecture provides a strategy for generating unique, chemically heterogeneous interfaces by synthesizing and utilizing analogs of **3CnCyTSH** for which the tailgroups in the adsorbates are compositionally distinct.

For the current set of cyclohexyl-based trithiols, the SAMs generated from these adsorbates were characterized by ellipsometry, contact angle goniometry, polarization modulation infrared reflection absorption spectroscopy (PM-IRRAS), and X-ray photoelectron spectroscopy (XPS). Analyses by XPS were also used to evaluate the thermal stability of the SAMs.

## EXPERIMENTAL SECTION

**Synthesis and Experimental Procedures.** The details of the synthesis of the tridentate cyclohexyl adsorbates, along with the materials used in their synthesis, the protocols for preparing the SAMs,

and the experimental procedures associated with the characterization of the SAMs, can be found in the Supporting Information.

## RESULTS AND DISCUSSION

**Ellipsometric Thickness Measurements.** Ellipsometry can be used to evaluate the average thickness of a self-assembled monolayer film and also trends within a series of SAMs.<sup>26</sup> For the films prepared in this study, the relative efficiency of the surface adsorption for these trithiol adsorbates or the possible formation of surface-bound disulfides, might noticeably distort the thickness measurements obtained for the resulting thin films.<sup>23,26</sup> Thus, with the current series of SAMs formed from the new adsorbates, we included that of the previously reported **3C1CyTSH** as a reference film. Comparison was also made to SAMs formed from *n*-octadecanethiol (**C18SH**), providing both a means of verifying the quality of our films and a standard for estimating the density of the surface chains for the new **3CnCyTSH** adsorbates.

The average ellipsometric thicknesses for the tridentate SAMs are  $\sim 4, 7, 10,$  and  $11 \text{ \AA}$  for **3C1CyTSH**, **3C3CyTSH**, **3C8CyTSH**, and **3C13CyTSH**, respectively, while that of the SAM generated from **C18SH** is  $\sim 21 \text{ \AA}$ . For the ellipsometric measurements of these new adsorbates, the carbon count used to equate these films with the total chain length of the normal alkanethiolate SAMs is equal to the alkyl chain substituent ( $R$ ) carbon count plus two carbons: the ring carbon and the carbon that links the thiol moiety to the ring. With the use of this methodology, the total chain lengths were 3, 5, 10, and 15 for **3C1CyTSH**, **3C3CyTSH**, **3C8CyTSH**, and **3C13CyTSH**, respectively. These data points are plotted in Figure 2 and

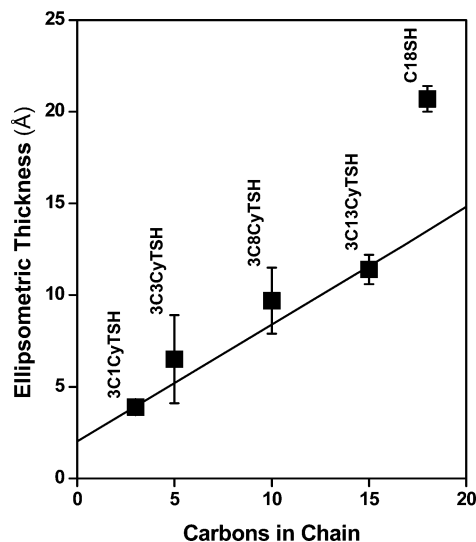


**Figure 2.** Ellipsometric thicknesses of the SAMs generated from **3CnCyTSH** and **C18SH**. Error bars indicate the variance associated with six measurements; standard deviations ranged from 0.3–2.4 Å. The solid line extending through the first four data points corresponds to a linear fit calculated for the **3CnCyTSH** SAM data and weighted for the associated standard deviations.

reveal that the new tridentate adsorbates generate monolayer films rather than multilayer films; as such, they likely offer the same characteristic features previously reported for the SAMs generated from **3C1CyTSH**.<sup>39</sup>

One observation from the plotted ellipsometric data is that the thicknesses of these films increase with increasing alkyl

chain length, and are in accord with the carbon counts for the total chain lengths for these adsorbates.<sup>40</sup> However, the data for the SAMs formed from 3C3CyTSH and 3C8CyTSH show a greater error associated with their measurements, which might indicate inconsistent or poorly formed films. The linear fit shown in Figure 2 was calculated from the first four data points (the tridentate adsorbates) utilizing the “error as weight” function in OriginPro 7.5. Using the standard equation for a line, the *y* intercept was determined to be  $\sim 2.0$  Å, and the increase in film thickness per each additional carbon atom in the alkyl chain (from the slope of the line) was  $\sim 0.6$  Å. The *y* intercept, a value attributable to the film thickness associated with the sulfur moieties present at the base of the adsorbates, is in line with previously reported values.<sup>41</sup> However, prior reports have provided calculated and empirically derived values for film thickness of  $\sim 1.2$ – $1.5$  Å per carbon for a normal alkanethiolate chain, yielding a conclusion that the chains for the 3C<sub>n</sub>CyTSH SAMs are either loosely packed or significantly tilted from surface normal.<sup>8</sup>

**XPS Analyses.** XPS is a useful method for determining the chemical compositions of SAMs. Additionally, the XPS spectra can be used to evaluate the effectiveness of the chemisorption of the sulfur headgroups to the gold substrate by monitoring the XPS binding energies. Minor differences between various S–Au bonds influences the distribution of electrons in the bonding orbitals of interest (reflecting the local environment), thus producing slight changes in the energy required to eject those electrons.<sup>42–44</sup> By monitoring the S<sub>2p</sub> region of the XPS spectra, the nature of the bonds formed (and the degree to which bonds fail to form) between the sulfur headgroups and the gold substrate can be obtained.<sup>43,44</sup> For the XPS spectra of SAMs generated from alkanethiols on gold, the binding energy (BE) of the S<sub>2p<sub>3/2</sub></sub> and S<sub>2p<sub>1/2</sub></sub> peaks for surface-bound thiols is known to be  $\sim 162.0$  and  $\sim 163.2$  eV, respectively. In contrast, the S<sub>2p<sub>3/2</sub></sub> and S<sub>2p<sub>1/2</sub></sub> peaks for unbound thiols (and disulfides) appear at  $\sim 164.0$  and  $\sim 165.2$  eV, respectively. Incomplete adsorbate bonding to gold, therefore, can be identified by the presence of an S<sub>2p</sub> peak at  $\sim 164$  eV and quantified by the deconvolution of the peaks in this region of the spectra. Moreover, oxidized sulfur species can also be detected by XPS (an S<sub>2p</sub> peak with BE > 166 eV).<sup>43,44</sup>

Previously,<sup>39</sup> we found that the SAMs derived from the adsorption of 3C1CyTSH from THF showed a high level of thiolate formation for these trithiols, with  $\sim 90\%$  of the sulfur atoms bound to gold as compared to the CyTSH-based SAMs, which displayed a markedly lower percentage of bound thiolate. Given the structural similarity of the new 3C<sub>n</sub>CyTSH adsorbates to 3C1CyTSH, we anticipated that the new adsorbates would also bind to gold with a high percentage of bound thiolate, a characteristic that might improve as the substituent alkyl chains are lengthened for these multidentate adsorbates, leaving little, if any, unbound thiol.

For purposes of comparison, the XPS spectrum for CyTSH is included in Figure 3 and shows that the SAMs formed from CyTSH are contaminated with oxidized sulfur species.<sup>39,43,44</sup> This adsorbate also exhibits a substantial amount of unbound sulfur as indicated by the peak at  $\sim 164$  eV, revealing that CyTSH either forms a disulfide upon partial bonding to the surface or adsorbs, leaving unbound thiols. In contrast, for the alkyl-substituted 3C<sub>n</sub>CyTSH adsorbates, there were no oxidized sulfur species present, as determined from the spectra, and the peaks associated with unbound thiol (and disulfide) were minimal.

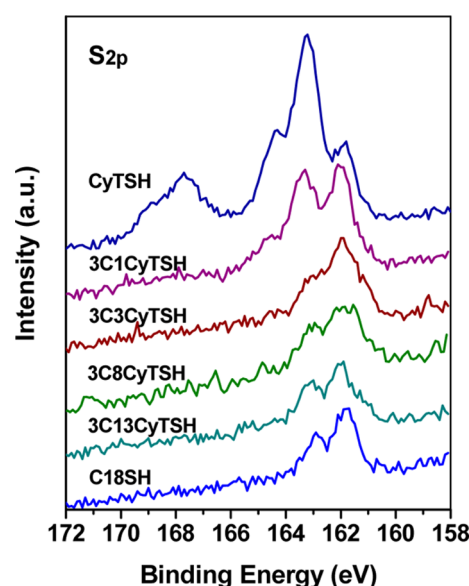


**Figure 3.** XPS spectra of the S<sub>2p</sub> region of the SAMs derived from the series of cyclohexyl-based tridentate adsorbates, 3C<sub>n</sub>CyTSH and CyTSH, compared to that of a C18SH SAM.

The relative amounts of bound and unbound sulfur were deconvoluted using standard XPS processing software; the deconvoluted spectra are provided in the Supporting Information. All of the peaks were fit with respect to spin–orbit splitting; specifically, two 80% Gaussian curves in a 1:2 ratio of areas split at 1.18 eV were used for analysis of the S<sub>2p</sub> peaks. The data obtained from this analysis are summarized in Table 1. The XPS data indicate a larger percentage of bound thiolate for the new adsorbates when compared to 3C1CyTSH.

**Table 1. Relative Amounts of Bound Versus Unbound Sulfur Species Obtained from Deconvolution of the XPS Spectra in Figure 3.<sup>a</sup>**

adsorbate	% bound thiolate	% unbound thiol
CyTSH	33	67 <sup>b</sup>
3C1CyTSH	65	35 <sup>b</sup>
3C3CyTSH	96	4
3C8CyTSH	100	0
3C13CyTSH	96	4
C18SH	100	0

<sup>a</sup>On the basis of these measurements, we estimate the accuracy of the reported percentages of bound versus unbound thiol to be no better than  $\pm 5\%$ . <sup>b</sup>Values were previously reported in ref 39.

In addition, the 3C3CyTSH, 3C8CyTSH, and 3C13CyTSH adsorbates show the highest percentage of bound thiolates and produce a statistically equivalent percentage of bound thiolates as C18SH. Analysis of the XPS data from the deconvolution of the peaks yields the following trend regarding the percentage of bound thiolate: C18SH  $\approx$  3C13CyTSH  $\approx$  3C8CyTSH  $\approx$  3C3CyTSH > 3C1CyTSH  $\gg$  CyTSH. Therefore, we conclude that, compared to 3C1CyTSH and CyTSH, the new tridentate adsorbates bind more completely to the surface of gold with all three sulfur atoms due to the presence of the longer alkyl chains on these adsorbates.

One possible rationalization for this phenomena is that the adsorbates adopt conformational structures that decrease the 1,3-diaxial interactions associated with the alkyl chains on the

**Table 2.** XPS Binding Energies,  $C_{1s}/Au_{4f}$  Ratios, and a Stoichiometric Comparison for SAMs Derived from the Indicated Adsorbates.<sup>a</sup>

adsorbate (molecular formula)	binding energy (eV)		$C_{1s} / Au_{4f}$ ratios	$C_{1s} / Au_{4f}$ per carbon	coverage comparison <sup>b</sup>
	$C_{1s}$	$S_{2p}$			
3C3CyTSH ( $C_{18}H_{36}S_3$ )	284.4	161.7	$1.85 \times 10^{-2}$	$1.03 \times 10^{-3}$	0.18
3C8CyTSH ( $C_{33}H_{66}S_3$ )	284.3	161.6	$2.34 \times 10^{-2}$	$7.09 \times 10^{-4}$	0.13
3C13CyTSH ( $C_{48}H_{96}S_3$ )	284.6	161.9	$4.71 \times 10^{-2}$	$9.81 \times 10^{-4}$	0.17
C18SH ( $C_{18}H_{38}S_1$ )	285.0	162.0	$1.01 \times 10^{-1}$	$5.61 \times 10^{-3}$	1.00

<sup>a</sup>Reflects the average values calculated from two independent measurements. The binding energies were referenced to  $Au_{4f7/2}$  at 84.0 eV.

<sup>b</sup>Normalized values of  $C_{1s}/Au_{4f}$  per carbon. Additional details can be found in the Supporting Information.

cyclohexane ring, which then creates favorable alignments of the *cis,cis*-trithiols on one side of the ring. These conformational effects lead to a more favorable adsorption to the surface of gold when compared to the thiol moieties of CyTSH. The bulkier the substituents, the greater the 1,3-diaxial interactions and the improved chemisorption of sulfur to gold. However, the alkyl chains of these adsorbates also tend to phase-associate in solution, with the van der Waals attractions of the longer alkyl chains increasing the likelihood of chain alignments on one side of the cyclohexane ring. Such a phase separation of nonpolar and polar groups on opposite sides of the ring can also encourage S–Au bonding by limiting the number of accessible cyclohexane ring conformers, or at least reducing the mobility of the substituents and thereby increasing the degree to which the thiol groups are oriented in the same direction.

XPS spectra can also be used to quantify the relative surface coverage of hydrocarbon adsorbates for a series of SAMs through an analysis of the ratio of the peak intensities for the  $C_{1s}$  and  $Au_{4f}$  signals.<sup>40,45</sup> An example of this approach can be found in research involving binary mixed-SAMs where the XPS C/Au ratio data was applied to determine the relative presence of the two components that produced the film.<sup>40</sup> Similar efforts on our part to use this ratio to characterize SAM films involve the analysis of a homologous series of alkanethiolate SAMs (even-numbered chains C8SH through C18SH) and produced a linear relationship for a plot of the C/Au ratio versus SAM thickness ( $r^2$  value of 0.98; see Figure S16 in the Supporting Information). Such trends reflect the fact that the consistent methodical addition of the same structural moiety to each homologous adsorbate in these series of SAMs produces an increase in the  $C_{1s}$  signal for the overlying hydrocarbon chains equivalent to the most attenuated carbon signal, the carbon next to the sulfur. However, from the perspective of how each additional methylene group contributes to the attenuation of signal for the existing structure (impact on escaping electrons), these added methylene groups can be considered as lying under the methyl group, exhibiting a proportional marginal impact upon the attenuation of signal for the existing hydrocarbon layer ( $C_{1s}$ ) as for the underlying gold ( $Au_{4f}$ ). Therefore, in our efforts to define the relative packing density of the adsorbed molecules of our newly developed series of SAMs, we chose to use the C/Au ratio to determine the relative surface coverage of the various adsorbates on gold.

Although the exact nature of the bonding of the trithiols to the surface of gold is unknown, we can examine the monolayer coverage of the cyclohexyl-based adsorbates normalized against the coverage of a normal alkanethiol SAM (see Table 2). To perform these estimations, the C/Au ratio for each of the SAMs was divided by the number of carbon atoms per adsorbate (based on their molecular formulas). The resulting C/Au ratio per carbon for each SAM was normalized with the C/Au ratio

per carbon for the C18SH SAM, providing an estimated stoichiometric surface coverage for each adsorbate.

As shown in Table 2, the relative coverages of the SAMs formed from 3C3CyTSH, 3C8CyTSH, and 3C13CyTSH were determined to be  $\sim 0.18$ , 0.13, and 0.17, respectively, as compared to 1.00 for the C18SH SAM. The data for 3C1CyTSH were not included in this analysis because of the high level of unbound thiol present in this SAM. Overall, our analysis indicates that the 3C3CyTSH and 3C13CyTSH adsorbates cover an area on the surface that is comparable to the area covered by  $\sim 5$ – $6$  alkanethiols, with the 3C8CyTSH SAM being more loosely packed (i.e.,  $\sim 7$ – $8$  alkanethiols). These values are consistent with a model in which the headgroups of these molecules are closely packed, given that each headgroup is comprised of a 1,3,5-trialkyl-substituted cyclohexyl ring oriented parallel to the surface.<sup>39</sup>

It is also possible to use the binding energies of the  $C_{1s}$  peaks in the XPS spectra to provide a qualitative evaluation of the relative packing density for a series of SAMs. In general, the BE of an electron in an atom will reflect both its chemical state and its environment.<sup>46</sup> Thus, the formation of bonds between atoms can change the electron distribution of the atom of interest, which can be evaluated by monitoring the shifts in BE from similarly structured SAMs. The relative insulating character of the samples is another factor that can influence the BE.<sup>46</sup> Previous studies of normal alkanethiolate SAMs have shown that the BE of the  $C_{1s}$  photoelectron shifts to a lower value when the alkyl chain length or packing density decreases.<sup>47,48</sup> This shift in BE has been rationalized on the basis of changes in the polarizability of the SAMs by assuming that the nature of the sulfur–gold interaction is unaffected by the length of the alkyl spacer. For example, the  $C_{1s}$  BE for a C18SH SAM is shifted to a lower energy when this SAM is partially decomposed or disordered due to the loosely packed SAM acting as a poor insulator.<sup>23</sup> Thus, the positive charges derived from the photoelectron emission can be more easily discharged by the partially decomposed loosely packed SAM than by the densely packed analogs. As a whole, the  $C_{1s}$  binding energy can be used to provide a rough estimate of the relative chain packing density for a series of compositionally similar SAMs.

Table 2 and Figure 4 show a small but reproducible shift of the  $C_{1s}$  peak to a lower binding energy for the 3CnCyTSH SAMs when compared to the densely packed C18SH SAM. The shift to lower binding energy for the 3C3CyTSH and 3C8CyTSH SAMs is notably larger ( $\Delta BE = \sim 0.7$  eV). From the observed shifts and the estimated coverage comparison, the relative alkyl chain packing density of the new cyclohexyl-based SAMs as compared to that formed from C18SH can be estimated as  $C18SH \gg 3C13CyTSH > 3C3CyTSH > 3C8CyTSH$ . We note, however, that the  $C_{1s}$  binding energy

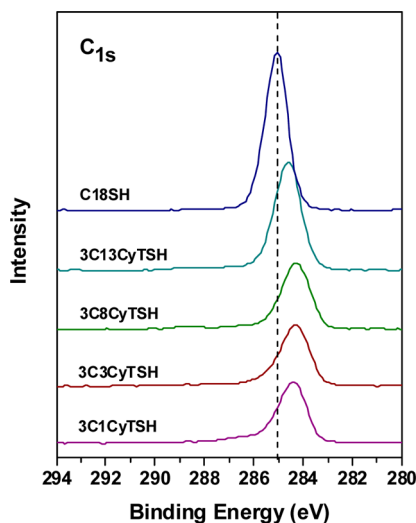


**Figure 4.** XPS spectra of the  $C_{1s}$  region of the SAMs derived from the series of cyclohexyl-based tridentate adsorbates,  $3C_n\text{CyTSH}$ , as compared to a SAM derived from **C18SH**. A dashed line is included to highlight the relative peak positions.

can be influenced by other factors, including the orientation of the alkyl chains.<sup>49</sup>

**PM-IRRAS Analyses.** The orientation and conformational order of self-assembled monolayer films can be evaluated by monitoring the C–H stretching region of the surface infrared spectra.<sup>42,50,51</sup> In particular, the frequency and bandwidth of the methylene antisymmetric and symmetric C–H stretching vibration bands ( $\nu_a^{\text{CH}_2}$  and  $\nu_s^{\text{CH}_2}$ ) are known to be strongly influenced by the conformational order and packing characteristics of hydrocarbon chains, such as those found in normal alkanes and alkanethiolate monolayers.

As shown in Figures 5 and 6, the  $\nu_a^{\text{CH}_2}$  bands of the SAMs derived from **3C3CyTSH**, **3C8CyTSH**, and **3C13CyTSH** appear at 2928, 2927, and 2926  $\text{cm}^{-1}$ , respectively, indicating a

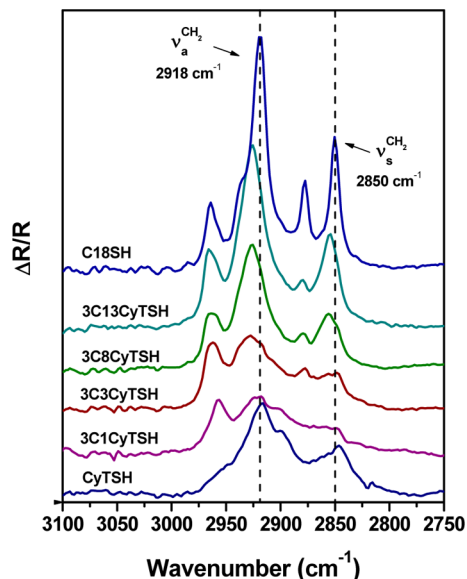


**Figure 5.** PM-IRRAS spectra of the series of SAMs formed from the new  $3C_n\text{CyTSH}$  adsorbates as compared to the spectra for the SAMs formed from **CyTSH** and **C18SH**. The dashed lines indicate the  $\nu_a^{\text{CH}_2}$  and  $\nu_s^{\text{CH}_2}$  band positions for the SAM derived from **C18SH**.

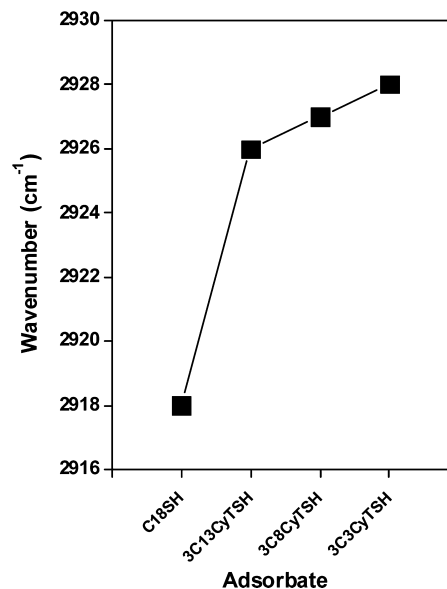


**Figure 6.** Average  $\nu_a^{\text{CH}_2}$  band position for the SAMs derived from **C18SH** and  $3C_n\text{CyTSH}$ , where  $n = 3, 8, 13$ . The line connecting the data points is provided solely as a guide to the eye.

conformationally disordered or liquidlike arrangement for the alkyl chains in these three SAMs. For comparison, the  $\nu_a^{\text{CH}_2}$  band of the SAM formed from **C18SH** appears at 2918  $\text{cm}^{-1}$ , which indicates a crystalline-like conformational order for the alkyl chains of this SAM.<sup>51</sup> A trend can be found in the data for the new  $3C_n\text{CyTSH}$  adsorbates: as the length of the alkyl tailgroups are lengthened, there is a slight increase in the conformational order of the SAMs, with the overall trend being **C18SH**  $\gg$  **3C13CyTSH** > **3C8CyTSH** > **3C3CyTSH**.

**Contact Angle Measurements.** For the current series of SAMs, the advancing contact angles ( $\theta_a$ ) were measured for several contacting liquids in contact with the SAMs derived from **3C3CyTSH**, **3C8CyTSH**, **3C13CyTSH**, and **C18SH**. The average values for the collected data are presented graphically in Figure 7. For this study, we chose liquids ranging from polar protic water ( $\text{H}_2\text{O}$ ) and formamide (FA) to slightly polar aprotic  $\alpha$ -bromonaphthalene ( $\alpha$ -BN) and nonpolar aprotic hexadecane (HD) to provide a more complete evaluation of the interfacial properties of the SAMs.<sup>40</sup> Due to the small molecular size of  $\text{H}_2\text{O}$  and FA, these probe liquids also tend to be highly sensitive to small changes in the interfacial packing of the chains that form these surfaces. Moreover, hexadecane serves as a particularly sensitive probe of the interfacial structure/packing of SAMs terminated with hydrocarbon tailgroups.<sup>40</sup>

The trends displayed in Figure 7 are consistent with trends found in the ellipsometric and PM-IRRAS data; specifically, the advancing contact angles increase progressively through the series from **3C3CyTSH** to **3C13CyTSH** as the films become less liquidlike and exhibit a maximum contact angle on the densely packed SAM formed from **C18SH**. A complete interpretation of the data is hindered by the confluence of at least two fundamental interactions: (1) the intercalation of the liquid molecules into the loosely packed alkyl chains, as exemplified by the complete wetting by HD but not the bulkier  $\alpha$ -BN molecules and (2) the interfacial energy of the liquids involved, as exemplified by the differences in the surface tensions of  $\text{H}_2\text{O}$  ( $\sim 73$  mN/m),<sup>52–54</sup> FA ( $\sim 58$  mN/m),<sup>54,55</sup>

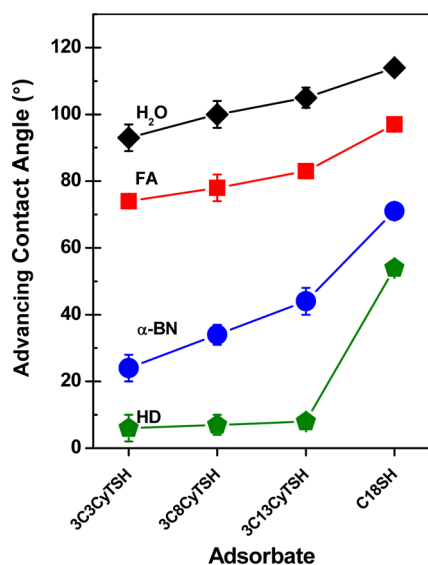


**Figure 7.** Advancing contact angles versus the adsorbate used to prepare the SAMs on gold for the new cyclohexyl-based tridentate adsorbates with alkyl chains as compared to a SAM formed from C18SH. H<sub>2</sub>O = water; FA = formamide;  $\alpha$ -BN =  $\alpha$ -bromonaphthalene; HD = hexadecane.

and  $\alpha$ -BN ( $\sim 45$  mN/m),<sup>56</sup> as juxtaposed to the resulting contact angles. Nevertheless, the trends indicate that the chain length of the 3CnCyTSH SAMs influences the contact angles, owing to the degree of conformational order for the alkyl chains, which increases with increasing chain length.<sup>51</sup>

**Preliminary Evaluation of the Thermal Stability of the New 3CnCyTSH SAMs.** Studies have shown that multidentate SAMs are more chemically and thermally stable than their corresponding monodentate analogs.<sup>11,12</sup> The enhanced stability can be rationalized largely on the basis of the chelate effect. Given this background, we anticipated that our new tridentate cyclohexyl-based thiol adsorbates would also form monolayers on gold that are more stable than normal alkanethiolate SAMs.

We used XPS to evaluate the thermal stability of the SAMs derived from the new 3CnCyTSH trithiols, utilizing the C18SH SAM as a standard.<sup>57</sup> In these studies, we monitored the peaks in the S<sub>2p</sub> region of the XPS spectra collected during the heating procedure outlined in the Experimental Section.

Notably, XPS survey spectra taken before the heating protocol are provided in the Supporting Information, and they indicate that the C18SH SAM and all of the 3CnCyTSH SAMs contain a small amount of adsorbed oxygen. The presence of this element within a SAM matrix has been credited with the degradation of SAM integrity either through direct attack on the headgroup or in a catalytic process involving “hot” electrons from the surface of gold.<sup>58</sup> Figure 8 shows the sulfur S<sub>2p</sub> spectra of SAMs generated on gold as a function of annealing temperature under vacuum. For the SAM formed from C18SH, a peak associated with oxidized sulfur (broad band at 167–170 eV) was observed upon completion of the heating protocol. The presence of this peak for this tightly packed film might reflect the barrier characteristics of the alkyl chains effectively blocking the escape of adsorbed oxygen from the matrix of the film. Further, the weak peak that appears in the same region in the final spectrum for 3C3CyTSH is so poorly resolved that it might simply reflect fluctuations in the baseline of the spectrum. As for SAMs formed from

3C8CyTSH and 3C13CyTSH, there is no indication of the formation of oxidized sulfur species in these films. Significantly, 3C13CyTSH showed a larger, better-defined bound thiolate peak than the SAM derived from 3C8CyTSH; a contrast that is apparent for each of the offsetting spectra in the two sets of collected data. However, this weakness in the intensity of the S<sub>2p</sub> peaks of the 3C8CyTSH SAMs during the heating protocol is also apparent in comparison to the data for the 3C3CyTSH SAMs and might reflect an inherent structural limitation associated with the intermediate alkyl chain length, where the chains are insufficiently long to create tightly packed chain assemblies and insufficiently short to act as noninteracting ring substituents. This potential rationalization is supported by some of the data presented above. For the XPS analysis of the surface density of the cyclohexyl-based SAMs, the SAM formed from 3C8CyTSH produced the lowest surface coverage of the new adsorbates. And one aspect of the PM-IRRAS data in Figure 5 also lends support to our conclusion; the peak for the methyl antisymmetric C–H stretching vibration ( $\nu_a^{\text{CH}_3}$ ) for the 3C8CyTSH SAM at  $\sim 2965$  cm<sup>-1</sup> is broader and less well-defined than that for the SAMs formed from 3C3CyTSH and 3C13CyTSH, which indicates that the terminal methyl groups are not uniformly oriented in the 3C8CyTSH SAM. However, most of the other collected instrumental data points to a general trend of increasing film order in tandem with increasing chain length for the substituent chains on the cyclohexyl rings.

On the basis of these preliminary thermal stability studies, we conclude that the formation of oxidized sulfur species within the SAM film under the conditions of our experimental procedures cannot be used as a general indicator of the thermal stability of these monolayers. The film that shows the greatest loss of signal in the XPS spectral region examined in this study was the SAM formed from 3C8CyTSH. The SAM formed from C18SH produced data indicating that a large number of the headgroups were oxidized during the heating protocol, yet the final spectrum also indicates that a substantial number of thiolate headgroups remain. Nevertheless, the best performing SAM in these preliminary studies of thermal stability appears to be the SAM formed from 3C13CyTSH. The enhanced stability can be partially attributed to the length of the overlying alkyl chains, which provide sufficient attractive van der Waals forces to form a better ordered film and also to the multiple bonds of these adsorbates to the surface of gold.<sup>17,20</sup>

## CONCLUSIONS

A series of tridentate adsorbates based on a trialkylcyclohexane structure supported by three methylthiol headgroups were synthesized and used to generate SAMs on gold. Thickness measurements obtained by ellipsometry indicate that the new SAMs exhibit reduced thicknesses as compared to alkanethiolate SAMs of comparable chain lengths. The conformational order for these SAMs as determined by the surface interactions with contacting liquids and the relative crystallinity of the alkyl chains as revealed by the PM-IRRAS spectra suggest an overall decreasing trend as follows: C18SH  $\gg$  3C13CyTSH > 3C8CyTSH > 3C3CyTSH. Characterization of the SAMs by XPS revealed that the sulfur atoms of the 3CnCyTSH tridentate adsorbates are bound to the surface of gold, and the alkyl tailgroups are loosely packed, with a notable reduction in chain packing density as compared to normal alkanethiolate SAMs. However, the molecular surface coverage of the trithiol SAMs, as calculated from the XPS data and the relative stoichiometries for the surface coverage of the molecules, are

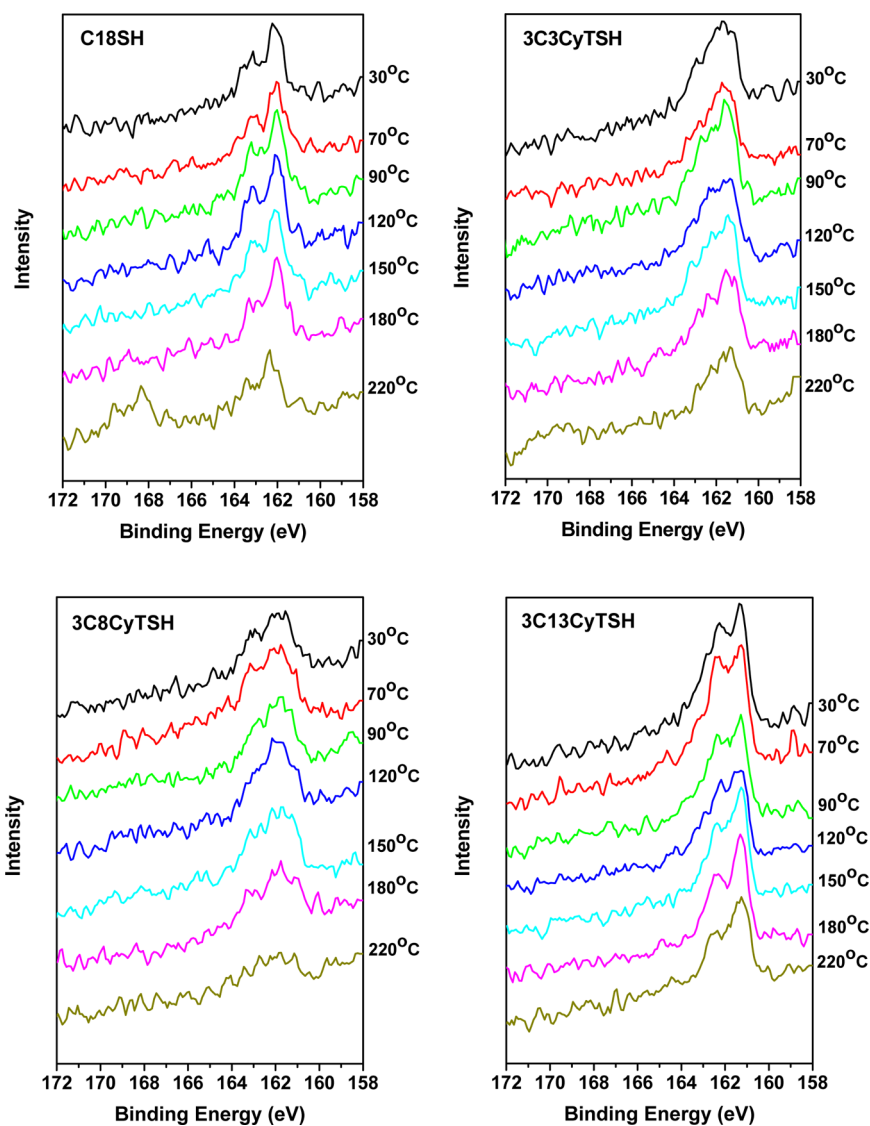


**Figure 8.** XPS spectra of the  $S_{2p}$  BE region of the SAMs derived from the new 3CnCyTSH trithiols and C18SH, collected after exposure to the indicated temperatures under vacuum.

consistent with a model in which the headgroups of the molecules are closely packed, given that each headgroup is comprised of a 1,3,5-trialkyl-substituted cyclohexyl ring oriented parallel to the surface. A preliminary study of the thermal stability of this series of SAMs shows that the SAM formed from 3C13CyTSH proved to be the most stable film under our experimental conditions, with the SAM formed from C18SH exhibiting significant headgroup oxidation during the heating protocol. The enhanced stability of the SAM formed from 3C13CyTSH was attributed to a combination of the stronger interchain van der Waals attractions associated with the longer overlying alkyl chains and the chelate effect.

## ■ ASSOCIATED CONTENT

### 📄 Supporting Information

Detailed synthesis procedures, materials used for synthesis and experimental work, experimental procedures for SAM characterization, XPS curve fitting protocol, curve-fitted spectra, and survey spectra for the 3CnCyTSH SAMs. This material is available free of charge via the Internet at <http://pubs.acs.org>.

## ■ AUTHOR INFORMATION

### Corresponding Author

\*E-mail: [trlee@uh.edu](mailto:trlee@uh.edu).

### Notes

The authors declare no competing financial interest.

## ■ ACKNOWLEDGMENTS

We thank the Robert A. Welch Foundation (Grant E-1320), the National Science Foundation (DMR-0906727), and the Texas Center for Superconductivity at the University of Houston for generous financial support.

## ■ REFERENCES

- (1) Kumar, A.; Abbott, N. L.; Kim, E.; Biebuyck, H. A.; Whitesides, G. M. Patterned Self-Assembled Monolayers and Meso-Scale Phenomena. *Acc. Chem. Res.* **1995**, *28*, 219–226.
- (2) Wilson, R. The Use of Gold Nanoparticles in Diagnostics and Detection. *Chem. Soc. Rev.* **2008**, *37*, 2028–2048.
- (3) Feng, F.; Sakoda, Y.; Ohyanagi, T.; Nagahori, N.; Shibuya, H.; Okamatsu, M.; Miura, N.; Kida, H.; Nishimura, S.-I. Novel Thiosialosides Tethered to Metal Nanoparticles as Potent Influenza

A Virus Haemagglutinin Blockers. *Antiviral Chem. Chemother.* **2013**, *23*, 59–65.

(4) Miozzo, L.; Yassar, A.; Horowitz, G. Surface Engineering for High Performance Organic Electronic Devices: The Chemical Approach. *J. Mater. Chem.* **2010**, *20*, 2513–2538.

(5) Maboudian, R.; Ashurst, W. R.; Carraro, C. Self-Assembled Monolayers as Anti-Stiction Coatings for MEMS: Characteristics and Recent Developments. *Sens. Actuators* **2000**, *82*, 219–223.

(6) Ulman, A. *An Introduction to Ultrathin Organic Films*; Academic: Boston, 1991.

(7) Love, J. C.; Estroff, L. A.; Kriebel, J. K.; Nuzzo, R. G.; Whitesides, G. M. Self-Assembled Monolayers of Thiolates on Metals as a Form of Nanotechnology. *Chem. Rev.* **2005**, *105*, 1103–1169.

(8) Bain, C. D.; Troughton, E. B.; Tao, Y. T.; Evall, J.; Whitesides, G. M.; Nuzzo, R. G. Formation of Monolayer Films by the Spontaneous Assembly of Organic Thiols from Solution onto Gold. *J. Am. Chem. Soc.* **1989**, *111*, 321–335.

(9) Delamar, E.; Michel, B.; Kang, H.; Gerber, Ch. Thermal Stability of Self-Assembled Monolayers. *Langmuir* **1994**, *10*, 4103–4108.

(10) Schoenfish, M. H.; Pemberton, J. E. Air Stability of Alkanethiol Self-Assembled Monolayers on Silver and Gold Surfaces. *J. Am. Chem. Soc.* **1998**, *120*, 4502–4513.

(11) Srisombat, L.; Jamison, A. C.; Lee, T. R. Stability: A Key Issue for Self-Assembled Monolayers on Gold as Thin-Film Coatings and Nanoparticle Protectants. *Colloids Surf., A* **2011**, *390*, 1–19.

(12) Chinwangso, P.; Jamison, A. C.; Lee, T. R. Multidentate Adsorbates for Self-Assembled Monolayer Films. *Acc. Chem. Res.* **2011**, *44*, 511–519.

(13) Garg, N.; Lee, T. R. Self-Assembled Monolayers Based on Chelating Aromatic Dithiols on Gold. *Langmuir* **1998**, *14*, 3815–3819.

(14) Willey, T. M.; Vance, A. L.; van Buuren, T.; Bostedt, C.; Terminello, L. J.; Fadley, C. S. Rapid Degradation of Alkanethiol-Based Self-Assembled Monolayers on Gold in Ambient Laboratory Conditions. *Surf. Sci.* **2005**, *576*, 188–196.

(15) Kim, T.; Chan, K. C.; Crooks, R. M. Polymeric Self-Assembled Monolayers. 4. Chemical, Electrochemical, and Thermal Stability of  $\omega$ -Functionalized, Self-Assembled Diacetylenic and Polydiacetylenic Monolayers. *J. Am. Chem. Soc.* **1997**, *119*, 189–193.

(16) Menzel, H.; Mowery, M. D.; Cai, M.; Evans, C. E. Vertical Positioning of Internal Molecular Scaffolding within a Single Molecular Layer. *J. Phys. Chem. B* **1998**, *102*, 9550–1055.

(17) Cai, M.; Mowery, M. D.; Pemberton, J. E.; Evans, C. E. Dual-Wavelength Resonance Raman Spectroscopy of Polydiacetylene Monolayers on Au Surfaces. *Appl. Spectrosc.* **2000**, *54*, 31–38.

(18) Menzel, H.; Horstmann, S.; Mowery, M. D.; Cai, M.; Evans, C. E. Diacetylene Polymerization in Self-Assembled Monolayers: Influence of the Odd/Even Nature of the Methylene Spacer. *Polymer* **2000**, *41*, 8113–8119.

(19) Shon, Y.-S.; Lee, T. R. A Steady-State Kinetic Model Can Be Used to Describe the Growth of Self-Assembled Monolayers (SAMs) on Gold. *J. Phys. Chem. B* **2000**, *104*, 8182–8191.

(20) Shon, Y.-S.; Colorado, R., Jr.; Williams, C. T.; Bain, C. D.; Lee, T. R. Low Density Self-Assembled Monolayers on Gold Derived from Chelating 2-Monoalkylpropane-1,3-dithiols. *Langmuir* **2000**, *16*, 541–548.

(21) Garg, N.; Carrasquillo-Molina, E.; Lee, T. R. Self-Assembled Monolayers Composed of Aromatic Thiols on Gold: Structural Characterization and Thermal Stability in Solution. *Langmuir* **2002**, *18*, 2717–2726.

(22) Park, J.-S.; Smith, A. C.; Lee, T. R. Loosely Packed Self-Assembled Monolayers on Gold Generated from 2-Alkyl-2-methylpropane-1,3-dithiols. *Langmuir* **2004**, *20*, 5829–5836.

(23) Park, J.-S.; Vo, A. N.; Barriet, D.; Shon, Y.-S.; Lee, T. R. Systematic Control of the Packing Density of Self-assembled Monolayers Using Bidentate and Tridentate Chelating Alkanethiols. *Langmuir* **2005**, *21*, 2902–2911.

(24) Zhang, S.; Leem, G.; Srisombat, L.; Lee, T. R. Rationally Designed Ligands that Inhibit the Aggregation of Large Gold Nanoparticles in Solution. *J. Am. Chem. Soc.* **2008**, *130*, 113–120.

(25) Nuzzo, R. G.; Allara, D. L. Adsorption of Bifunctional Organic Disulfides on Gold Surfaces. *J. Am. Chem. Soc.* **1983**, *105*, 4481–4483.

(26) Nuzzo, R. G.; Fusco, F. A.; Allara, D. L. Spontaneously Organized Molecular Assemblies. 3. Preparation and Properties of Solution Adsorbed Monolayers of Organic Disulfides on Gold Surfaces. *J. Am. Chem. Soc.* **1987**, *109*, 2358–2368.

(27) Whitesell, J. K.; Chang, H. K. Directionally Aligned Helical Peptides on Surfaces. *Science* **1993**, *261*, 73–76.

(28) Fox, M. A.; Whitesell, J. K.; McKerrow, A. J. Fluorescence and Redox Activity of Probes Anchored through an Aminotrithiol to Polycrystalline Gold. *Langmuir* **1998**, *14*, 816–813.

(29) Schmitt, H.; Badia, A.; Dickinson, L.; Reven, L.; Lennox, R. B. The Effect of Terminal Hydrogen Bonding on the Structure and Dynamics of Nanoparticle Self-Assembled Monolayers (SAMs): An NMR Dynamics Study. *Adv. Mater.* **1998**, *10*, 475–480.

(30) Mosley, D. W.; Sellmyer, M. A.; Daida, E. J.; Jacobson, J. M. Polymerization of Diacetylenes by Hydrogen Bond Templated Adlayer Formation. *J. Am. Chem. Soc.* **2003**, *125*, 10532–10533.

(31) Ferguson, M. K.; Lohr, J. R.; Day, B. S.; Morris, J. R. Influence of Buried Hydrogen-Bonding Groups within Monolayer Films on Gas-Surface Energy Exchange and Accommodation. *Phys. Rev. Lett.* **2004**, *92*, 073201–073204.

(32) Shon, Y.-S.; Lee, T. R. Chelating Self-Assembled Monolayers on Gold Generated from Spiroalkanedithiols. *Langmuir* **1999**, *15*, 1136–1140.

(33) Srisombat, L.; Park, J. -S.; Zhang, S.; Lee, T. R. Preparation, Characterization, and Chemical Stability of Gold Nanoparticles Coated with Mono-, Bis-, and Tris-Chelating Alkanethiols. *Langmuir* **2008**, *24*, 7750–7754.

(34) Katano, S.; Kim, Y.; Kitagawa, T.; Kawai, M. Tailoring Electronic States of a Single Molecule Using Adamantane-based Molecular Tripods. *Phys. Chem. Chem. Phys.* **2013**, *15*, 14229–14233.

(35) Kittredge, K. W.; Minton, M. A.; Fox, M. A.; Whitesell, J. K.  $\alpha$ -Helical Polypeptide Films Grown from Sulfide or Thiol Linkers on Gold Surfaces. *Helv. Chim. Acta* **2002**, *85*, 788–798.

(36) Kitagawa, T.; Idomoto, Y.; Matsubara, H.; Hobara, D.; Kakiuchi, T.; Okazaki, T.; Komatsu, K. Rigid Molecular Tripod with an Adamantane Framework and Thiol Legs. Synthesis and Observation of an Ordered Monolayer on Au(111). *J. Org. Chem.* **2006**, *71*, 1362–1369.

(37) Katano, S.; Kim, Y.; Matsubara, H.; Kitagawa, T.; Kawai, M. Hierarchical Chiral Framework Based on a Rigid Adamantane Tripod on Au(111). *J. Am. Chem. Soc.* **2007**, *129*, 2511–2515.

(38) Kitagawa, T.; Matsubara, H.; Komatsu, K.; Hirai, K.; Okazaki, T.; Hase, T. Ideal Redox Behavior of the High-Density Self-Assembled Monolayer of a Molecular Tripod on a Au(111) Surface with a Terminal Ferrocene Group. *Langmuir* **2013**, *29*, 4275–4282.

(39) Singhana, B.; Rittikulsittichai, S.; Lee, T. R. Tridentate adsorbates with cyclohexyl headgroups assembled on gold. *Langmuir* **2013**, *29*, 561–569.

(40) Bain, C. D.; Whitesides, G. M. Formation of Monolayers by the Coadsorption of Thiols on Gold: Variation in the Length of the Alkyl Chain. *J. Am. Chem. Soc.* **1989**, *111*, 7164–7175.

(41) Miura, Y. F.; Takenaga, M.; Koini, T.; Graupe, M.; Garg, N.; Graham, R. L., Jr.; Lee, T. R. Wettabilities of Self-Assembled Monolayers Generated from CF<sub>3</sub>-Terminated Alkanethiols on Gold. *Langmuir* **1998**, *14*, 5821–5825.

(42) Laibinis, P. E.; Whitesides, G. M.; Allara, D. L.; Tao, Y. T.; Parikh, A. N.; Nuzzo, R. G. Comparison of the Structures and Wetting Properties of Self-Assembled Monolayers of *n*-Alkanethiols on the Coinage Metal Surfaces, Copper, Silver, and Gold. *J. Am. Chem. Soc.* **1991**, *113*, 7152–7167.

(43) Castner, D. G.; Hinds, K.; Grainger, D. W. X-ray Photoelectron Spectroscopy Sulfur 2p Study of Organic Thiol and Disulfide Binding Interactions with Gold Surfaces. *Langmuir* **1996**, *12*, 5083–5086.

(44) Duwez, A.-S. Exploiting Electron Spectroscopies to Probe the Structure and Organization of Self-Assembled Monolayer: A Review. *J. Electron Spectrosc. Relat. Phenom.* **2004**, *134*, 97–138.

(45) Folkers, J. P.; Laibinis, P. E.; Whitesides, G. M. Self-assembled Monolayers of Alkanethiols on Gold: Comparisons of Monolayers Containing Mixtures of Short- and Long-Chain Constituents with Methyl and Hydroxymethyl Terminal Groups. *Langmuir* **1992**, *8*, 1330–1341.

(46) Vickerman, J. C. *Surface Analysis: The Principal Techniques*, 1st Ed.; John Wiley & Sons: Chichester, West Sussex, England, 1997.

(47) Biebuyck, H. A.; Bain, C. D.; Whitesides, G. M. Comparison of Organic Monolayers on Polycrystalline Gold Spontaneously Assembled from Solutions Containing Dialkyl Disulfides or Alkanethiols. *Langmuir* **1994**, *10*, 1825–1831.

(48) Ishida, T.; Hara, M.; Kojima, I.; Tsuneda, S.; Nishida, N.; Sasabe, H.; Knoll, W. High Resolution X-ray Photoelectron Spectroscopy Measurements of Octadecanethiol Self-Assembled Monolayers on Au(111). *Langmuir* **1998**, *14*, 2092–2096.

(49) Himmel, H. J.; Woell, C.; Gerlach, R.; Polanski, G.; Rubahn, H. G. Structure of Heptanethiolate Monolayers on Au(111): Adsorption from Solution vs Vapor Deposition. *Langmuir* **1997**, *13*, 602–605.

(50) Snyder, R. G.; Strauss, H. L.; Elliger, C. A. Carbon-Hydrogen Stretching Modes and the Structure of n-Alkyl Chains. I. Long, Disordered Chains. *J. Phys. Chem.* **1982**, *86*, 5145–5150.

(51) Porter, M. D.; Bright, T. B.; Allara, D. L.; Chidsey, C. E. D. Spontaneously Organized Molecular Assemblies. 4. Structural Characterization of n-Alkyl Thiol Monolayers on Gold by Optical Ellipsometry, Infrared Spectroscopy, and Electrochemistry. *J. Am. Chem. Soc.* **1987**, *109*, 3559–3568.

(52) Fowkes, F. M.; Riddle, F. L., Jr.; Pastore, W. E.; Weber, A. A. Interfacial Interactions Between Self-Associated Polar Liquids and Squalane Used to Test Equations for Solid-Liquid Interfacial Interactions. *Colloids Surf.* **1990**, *43*, 367–387.

(53) Smallwood, I. M. *Handbook of Organic Solvent Properties*; John Wiley & Sons: New York, 1996.

(54) Weinbach, S. P.; Kjaer, K.; Als-Nielsen, J.; Lahav, M.; Leiserowitz, L. Self-Assembled Langmuir Monolayers and Trilayers at the Air-Formamide Interface. *J. Phys. Chem.* **1993**, *97*, 5200–5203.

(55) Saint-Jalmesa, A.; Gallet, F. Buckling in a Solid Langmuir Monolayer: Light Scattering Measurements and Elastic Model. *Eur. Phys. J. B* **1998**, *2*, 489–494.

(56) Good, R. J.; Elbing, E. Generalization of Theory for Estimation of Interfacial Energies. *Ind. Eng. Chem.* **1970**, *62*, 54–59.

(57) Büttner, M.; Belsler, T.; Oelhafen, P. Stability of Thiol-Passivated Gold Particles at Elevated Temperatures Studied by X-ray Photoelectron Spectroscopy. *J. Phys. Chem. B* **2005**, *109*, 5464–5467.

(58) Huang, J.; Hemminger, J. C. Photooxidation of Thiols in Self-Assembled Monolayers on Gold. *J. Am. Chem. Soc.* **1993**, *115*, 3342–3343.